Time-Dependent, Multi-Wavelength Models for Active Flares of Fermi Blazars

Matthew G. Baring,[1] Markus Boettcher,[2] *and* Errol J. Summerlin[3]

[1]Rice University, [2]North-West University Potchefstroom,
[3]NASA's Goddard Space Flight Center

[1]baring@rice.edu

Fermi Symposium, Baltimore, MD, October 16th 2018

Confined Acceleration + Radiation Zones

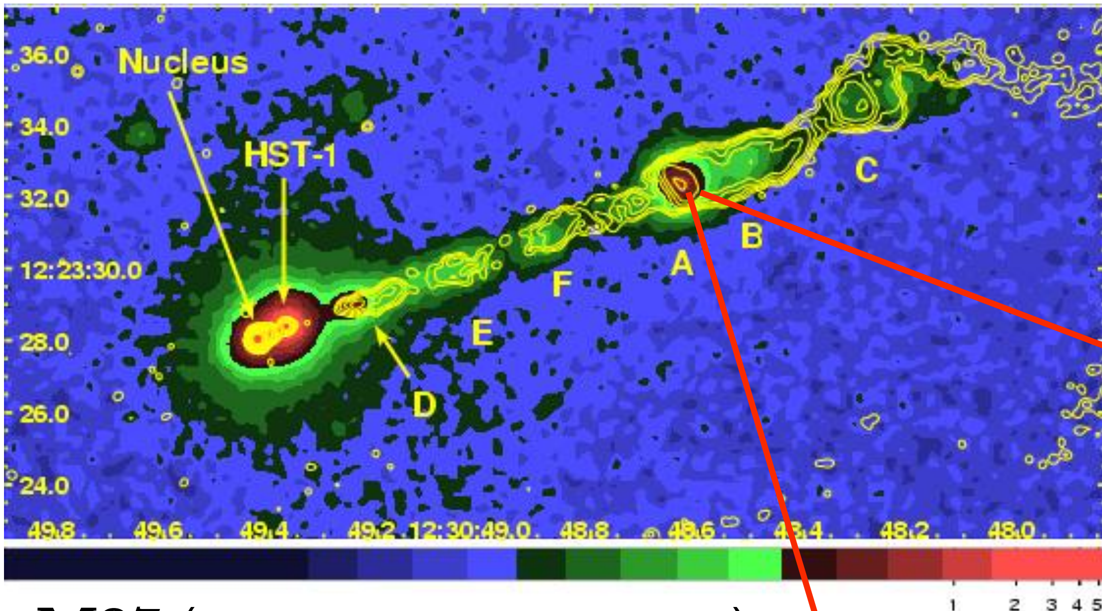

M87 (Harris & Krawczynski 2006)

Two-zone

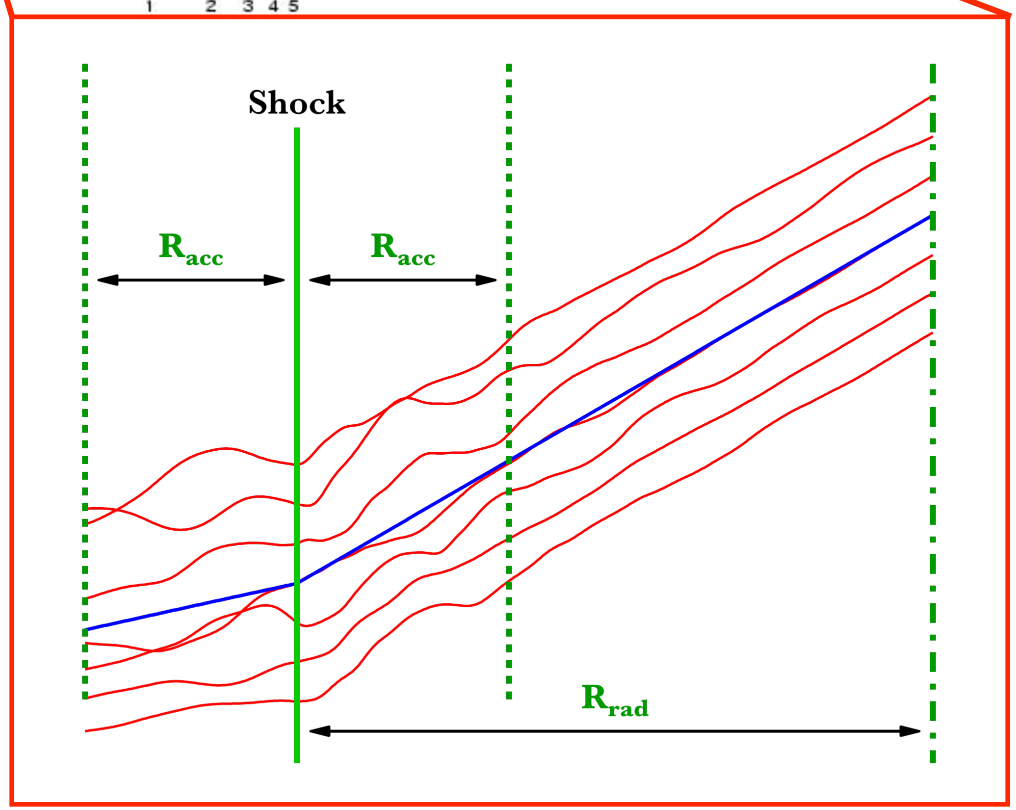

- *Right*: Schematic of our blazar model geometry, consisting of a region proximate to the shock that is the acceleration (injection) zone which is embedded in a much larger radiation zone.
- Also depicted is a turbulent field, signified by the red field line projections.

Numerical Scheme

- Injection spectra $Q_e(\gamma,t')$ from turbulence characteristics + MC simulations of DSA
- Injection from small acceleration zone (shock) into larger radiation zone
- Time-dependent leptonic code based on Böttcher & Chiang (2002)
- Radiative processes:
  - Synchrotron
  - Synchrotron self-Compton (SSC)
  - External Compton (EC: dust torus + BLR + direct accretion disk)

Shock injection "on"
for
$0 < \Delta t' < L'/v'_s$

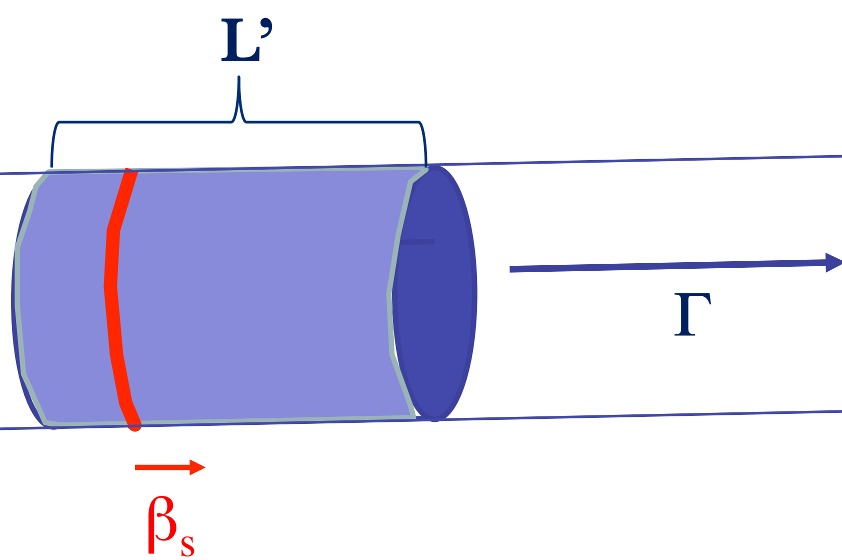

$Q_e(\gamma,t') = Q_e(\gamma)\ H(t';\ 0,\ Dt')$, primes denoting comoving jet frame.

Time-Dependent Electron Evolution with Radiative Energy Losses

The **acceleration timescale for electrons is short**: it scales as the cyclotron period (for shock drift and diffusive acceleration):

$$t_{\rm acc} \sim \eta\, t_{\rm cyc} = \eta\, \frac{2\pi\gamma\beta m_e c}{eB} \ll t_{\rm cool}\, ,\; t_{\rm dyn}$$

for most electrons, i.e. those below around 300 MeV in blazars.

- For time evolution of blazar flares, we therefore use a shock-acceleration electron distribution (from Summerlin & Baring 2012) as an **instantaneous injection** $Q_e(\gamma)$.
- Then **solve a Fokker-Planck equation** for electron distribution evolution in the jet frame:

$$\frac{\partial n_e}{\partial t'} = -\frac{\partial}{\partial\gamma}\Bigl(\dot{\gamma} n_e\Bigr) + Q_e(\gamma,\, t') - \frac{n_e}{t_{\rm esc}} \quad \text{for} \quad n_e \equiv n_e(\gamma,\, t')\, .$$

This includes competition between acceleration and cooling.

One-zone Multiwavelength SSC fits to BL Lacertae

Baring, Böttcher & Summerlin (MNRAS 464, 4875, 2017)

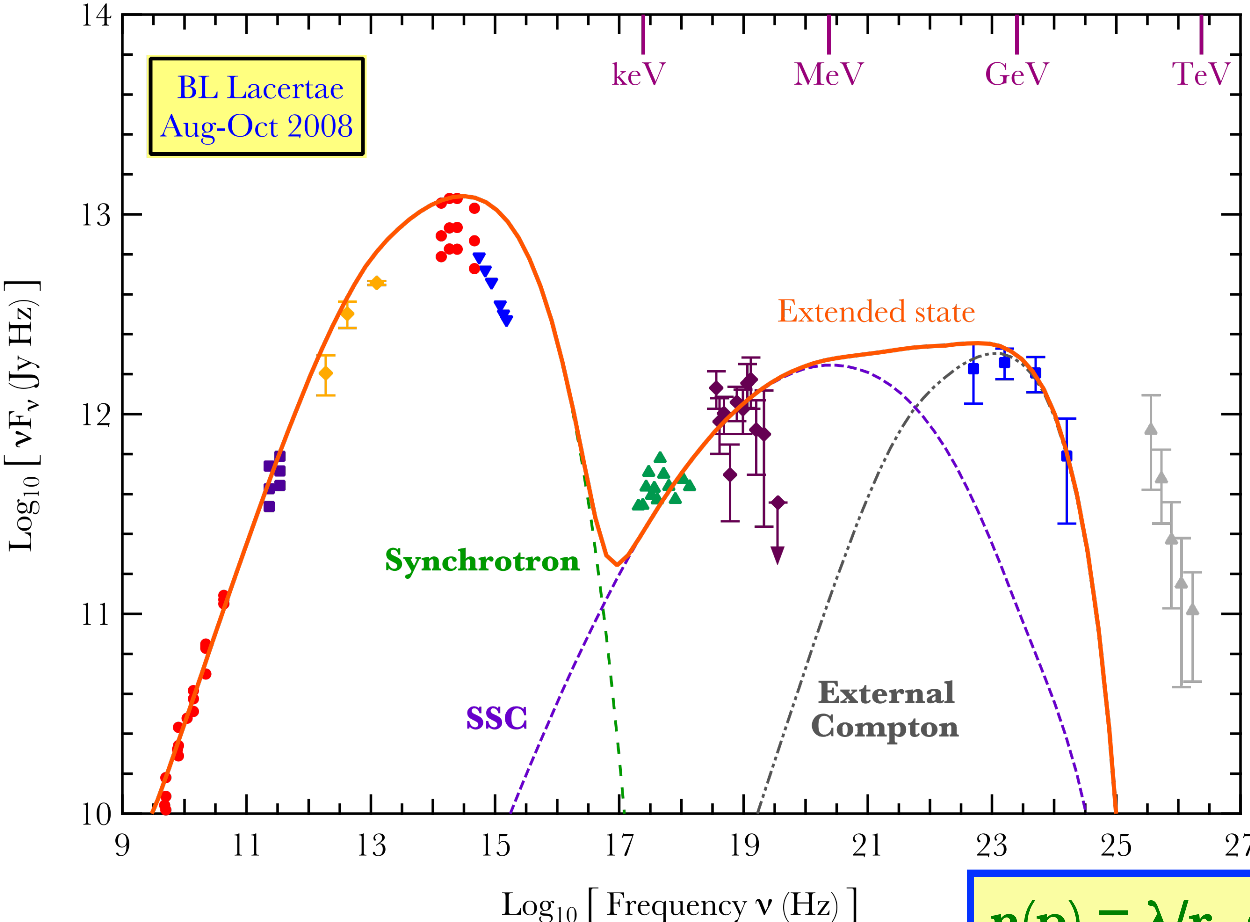

z=0.069

η_1=20
α=3

$\eta(p) = \lambda/r_g \sim \eta_1 \, (p/mc)^{\alpha-1}$

- SSC explains X-rays but cannot fit gamma-rays; EC component added.
- Large η ($\sim 10^7$) needed to move synchrotron peak into optical (for LBLs).

FSRQ 3C279

Extended flaring period 2013 – 2014

Variability time scale ~ 1 day

(Hayashida et al. 2015)

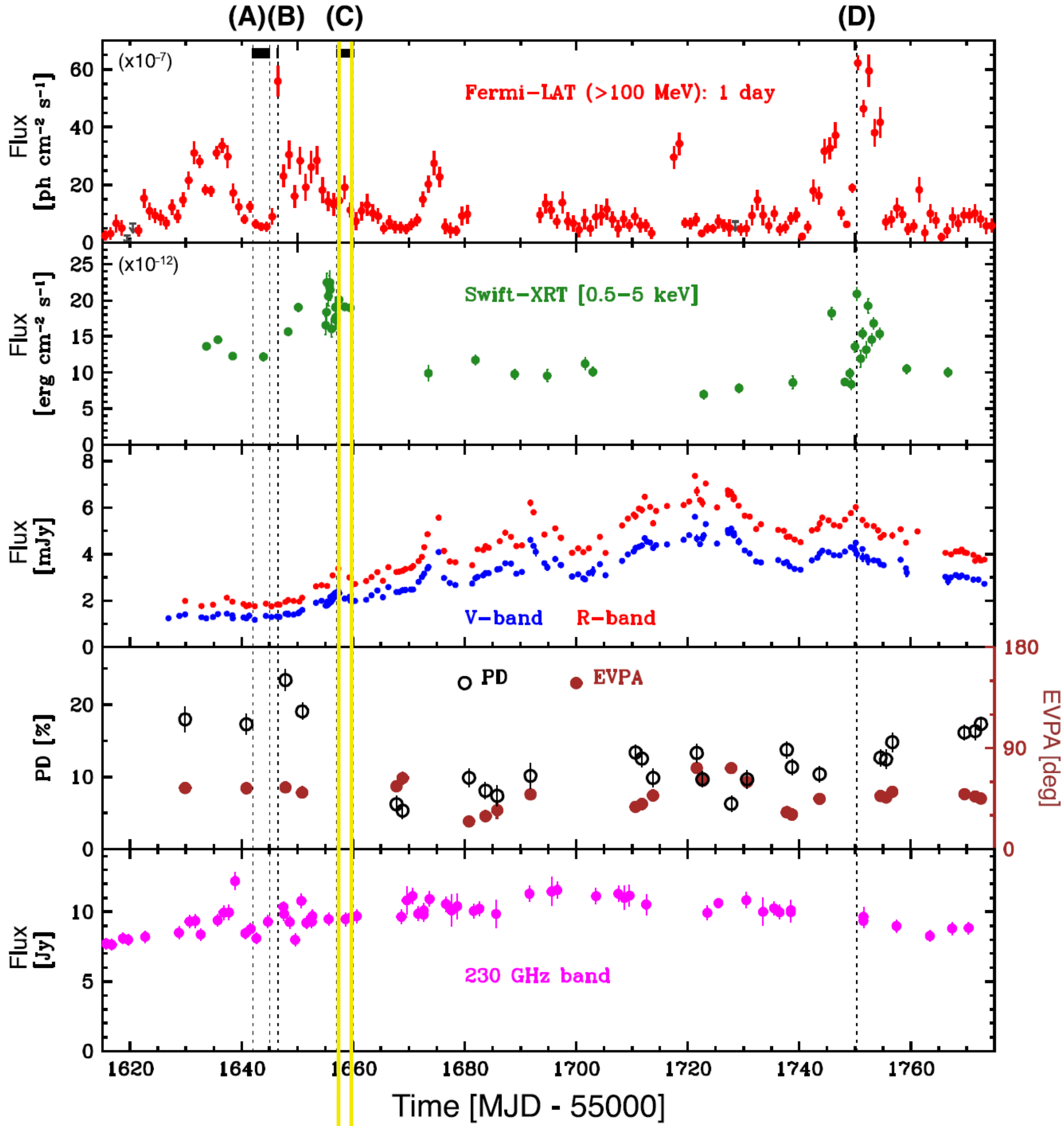

Shock Injected and Cooled Electrons

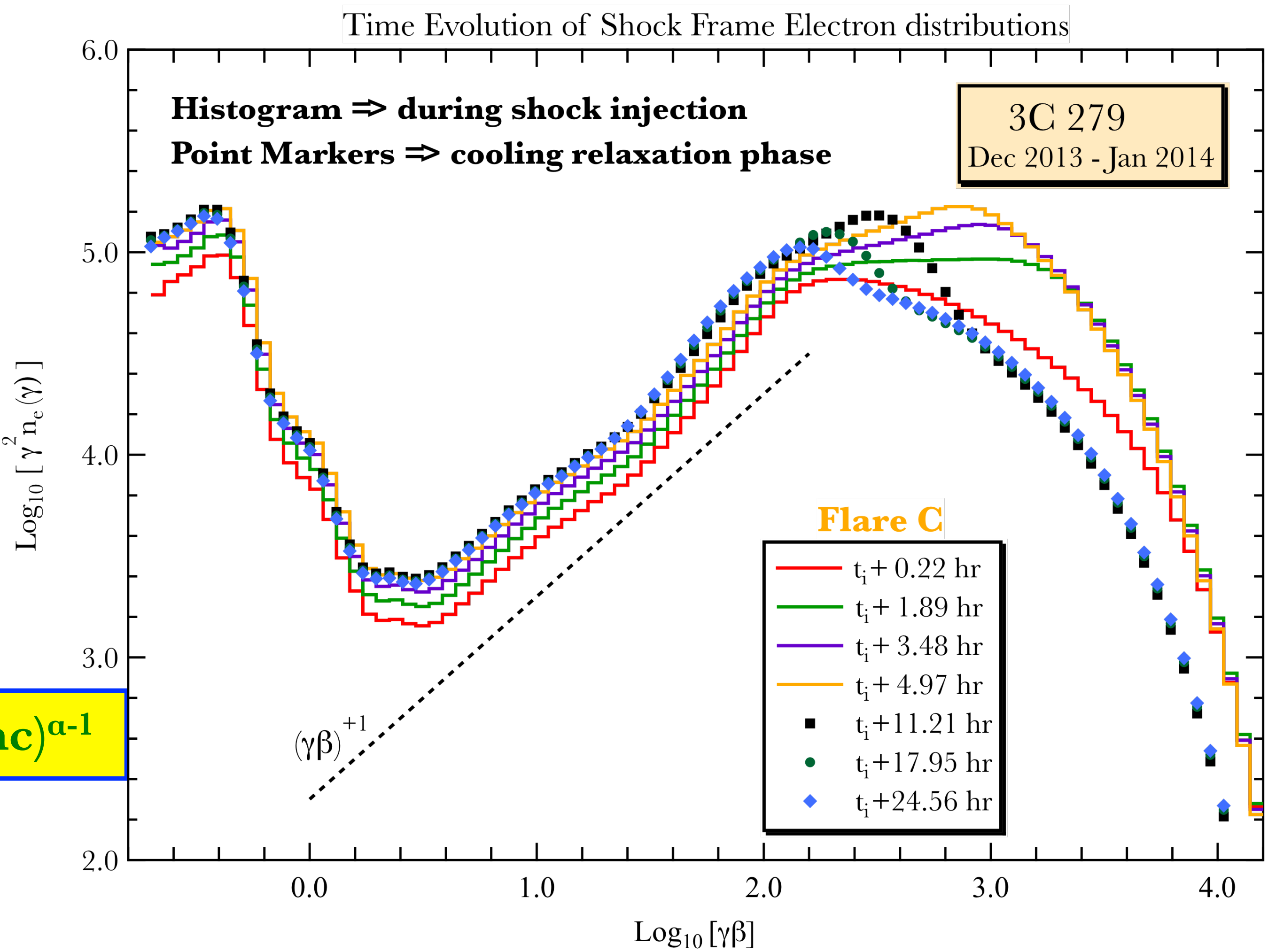

$\eta(p) = \lambda/r_g \sim \eta_1\,(p/mc)^{\alpha-1}$

- The non-thermal particle spectral index and thermal-to-non-thermal normalization from Monte Carlo acceleration simulations are strongly dependent on η_1 (=100 in the figure) and α (=3 in figure).

Evolving MW Spectra during 3C 279 flares – Dec 2013-Apr 2014

- Time evolution of MW spectra for 3C 279 during strong flares in January 2014.
- Model curves are derived for flare C only, with different times during a flare corresponding to different colors and linestyles.

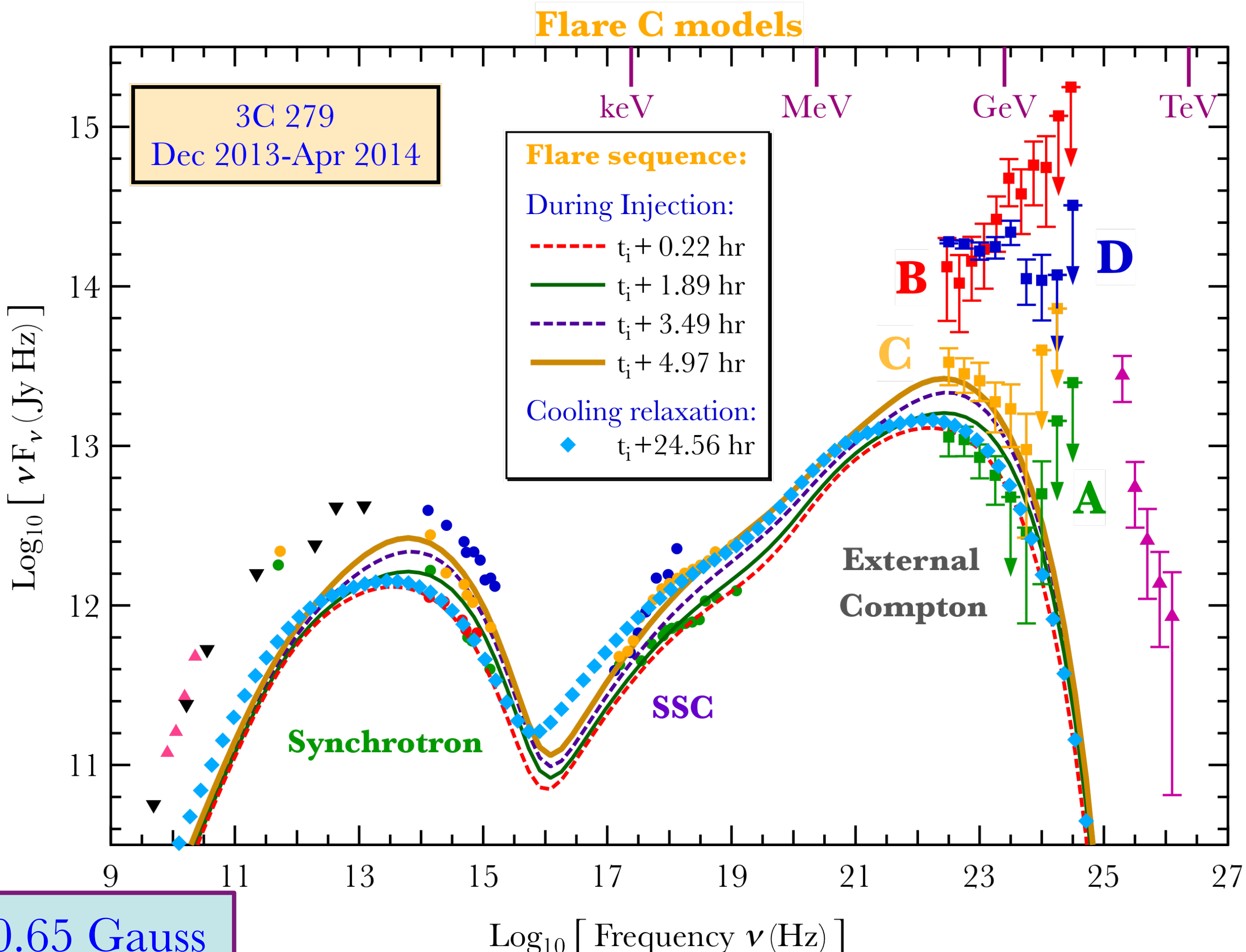

Γ=15, B'=0.65 Gauss

3C 279: Time Evolution Models for Flare C

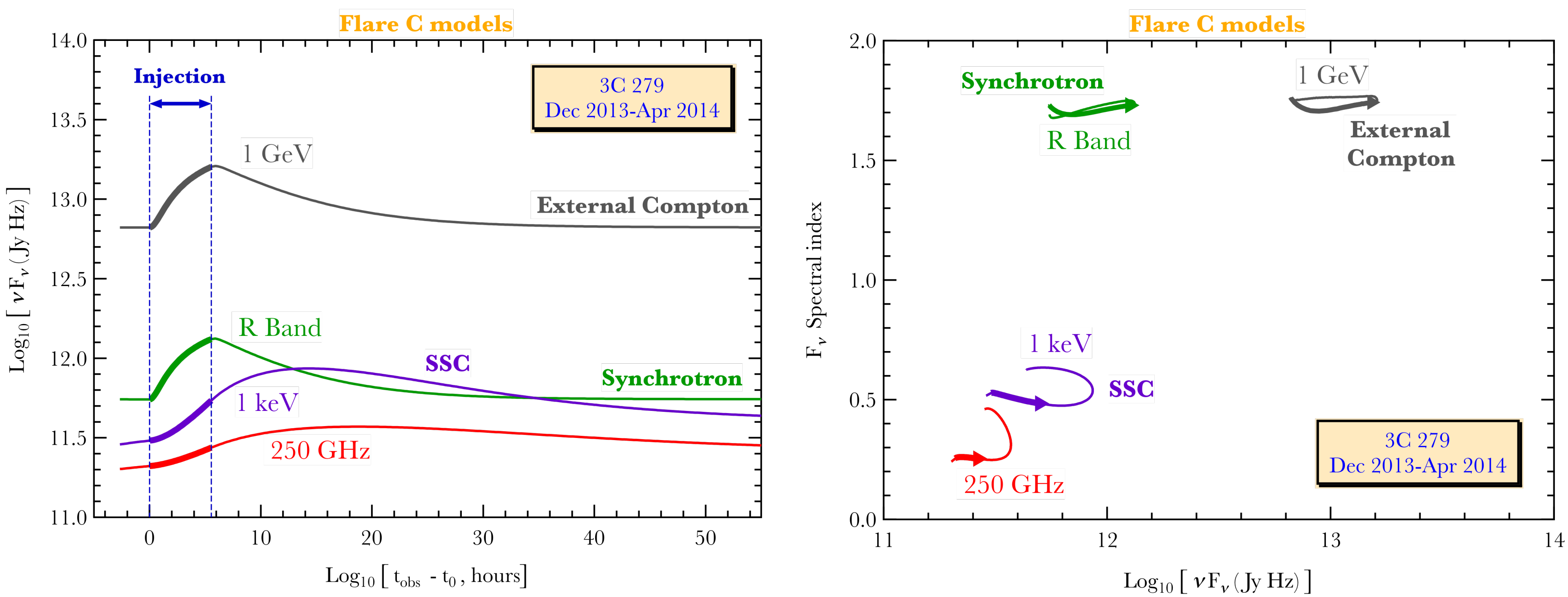

- *Left panel*: Model time traces of νF_ν fluxes displaying various delays in radio to gamma-ray wavebands during Flare C. Onset of injection is at t=0.
- *Right panel*: Evolutionary traces in the spectral index/flux plane with time directions as indicated. The different wavebands are labeled by their components: synchrotron, SSC and external Compton. Spectral hysteresis assumes a characteristic counter-clockwise form.

3C 279: *Fermi*-LAT light curves

- Periods B and D suggest possibly asymmetric injection of duration close to GeV cooling timescales (1-3 hours)
- Hayashida et al. (2015, ApJ 807:79)

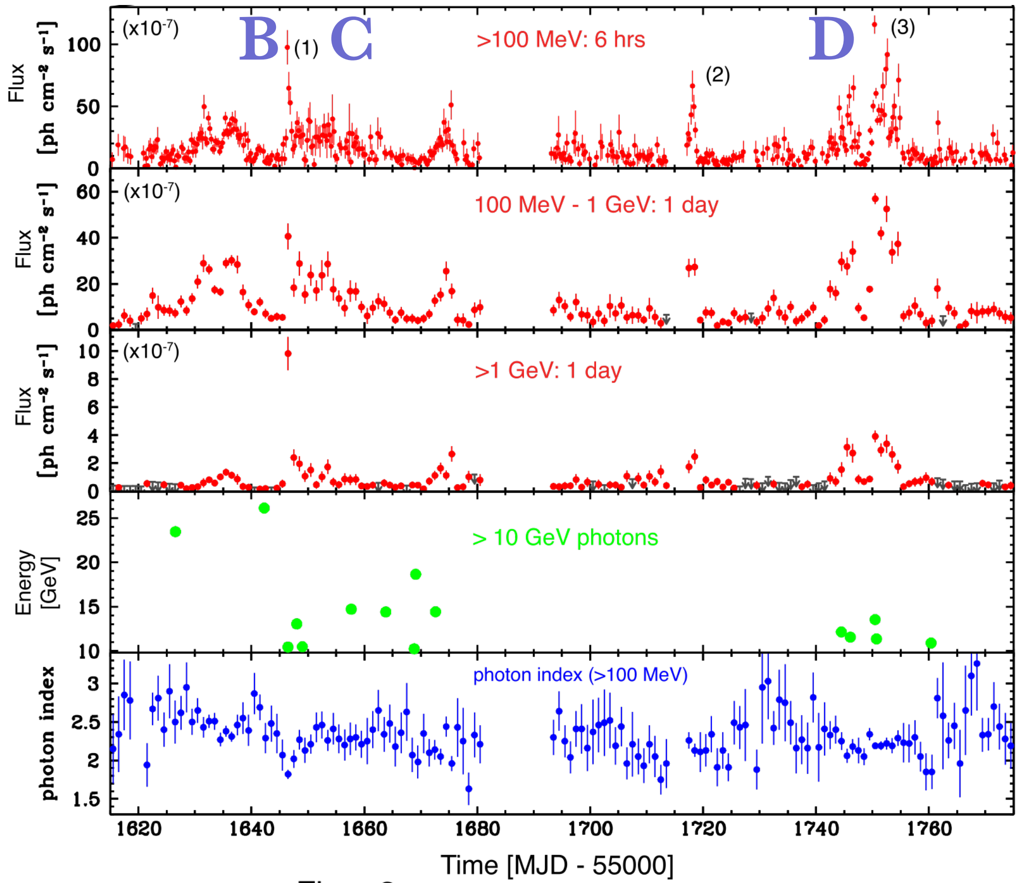

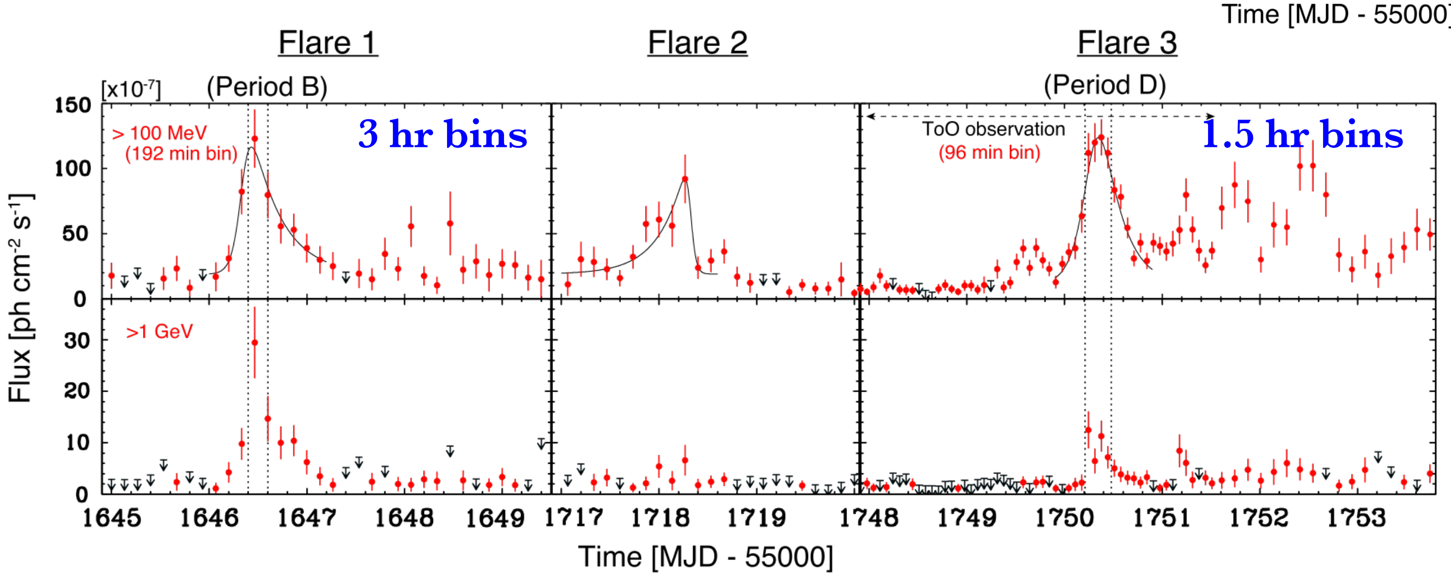

Conclusions

- **Broadband blazar spectra: X-ray/γ-ray diagnostics on turbulence power spectra and particle diffusion.**
  - Details in Baring, Böttcher & Summerlin (MNRAS 464, 4875, 2017)
- **Coupled Monte Carlo Simulations of diffusive shock acceleration and radiation transport reveal strongly energy-dependent mean-free-path to scattering.**
  - **MW fits demand $\eta=\lambda/r_g$ to be an increasing function of p as scales sample greater distances from the shock.**
- **3C 279 (an LBL) presents a particular temporal case:**
  - **Hardness/flux evolution displays characteristic counter-clockwise spectral hysteresis in all bands.**
  - **X-rays and radio are well-correlated, but lag optical and γ-rays by about 5-9 hours. => comparative cooling times.**
  - **Different lags/hysteresis are expected for other blazar types.**
- **Spectroscopy and evolution present consistency in model parameter determination.**
- **Next test: modeling hard *Fermi*-LAT Flare B.**

3C279 – Flare C
Discrete Correlation Functions

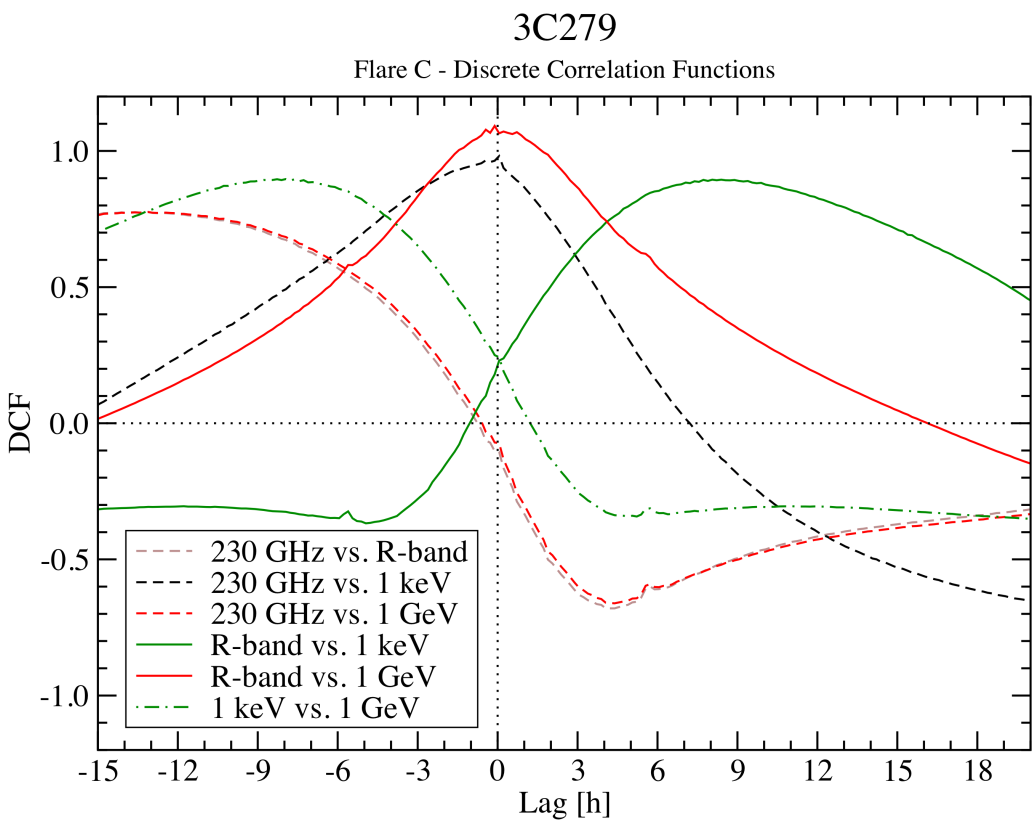

The discrete correlation function is

$$\mathcal{C}_{a,b}(\tau) \;\equiv\; \frac{1}{\mathcal{N}_a \mathcal{N}_b} \int_{-\infty}^{\infty} \mathcal{F}_a(t)\, \mathcal{F}_b(\tau - t)\, dt$$

for fluxes $\mathcal{F}_{a,b}$ in wavebands a,b, with

$$\mathcal{N}_a \;=\; \int_{-\infty}^{\infty} \mathcal{F}_a(t)\, dt$$

defining the normalizations.

After Edelson & Krolik (1988, ApJ **333**, 646).

- **DCF** measures relative fluxes between different bands.
- Optical and γ-rays **well correlated** (0 lag). X-rays and radio **well correlated** (0 lag).
- X-rays and radio **lag** optical + γ-rays by **5-9 hrs**, latter being generated by higher energy electrons, and therefore possessing a shorter response (cooling) time.

One-zone Multiwavelength SSC fits to Mrk 501

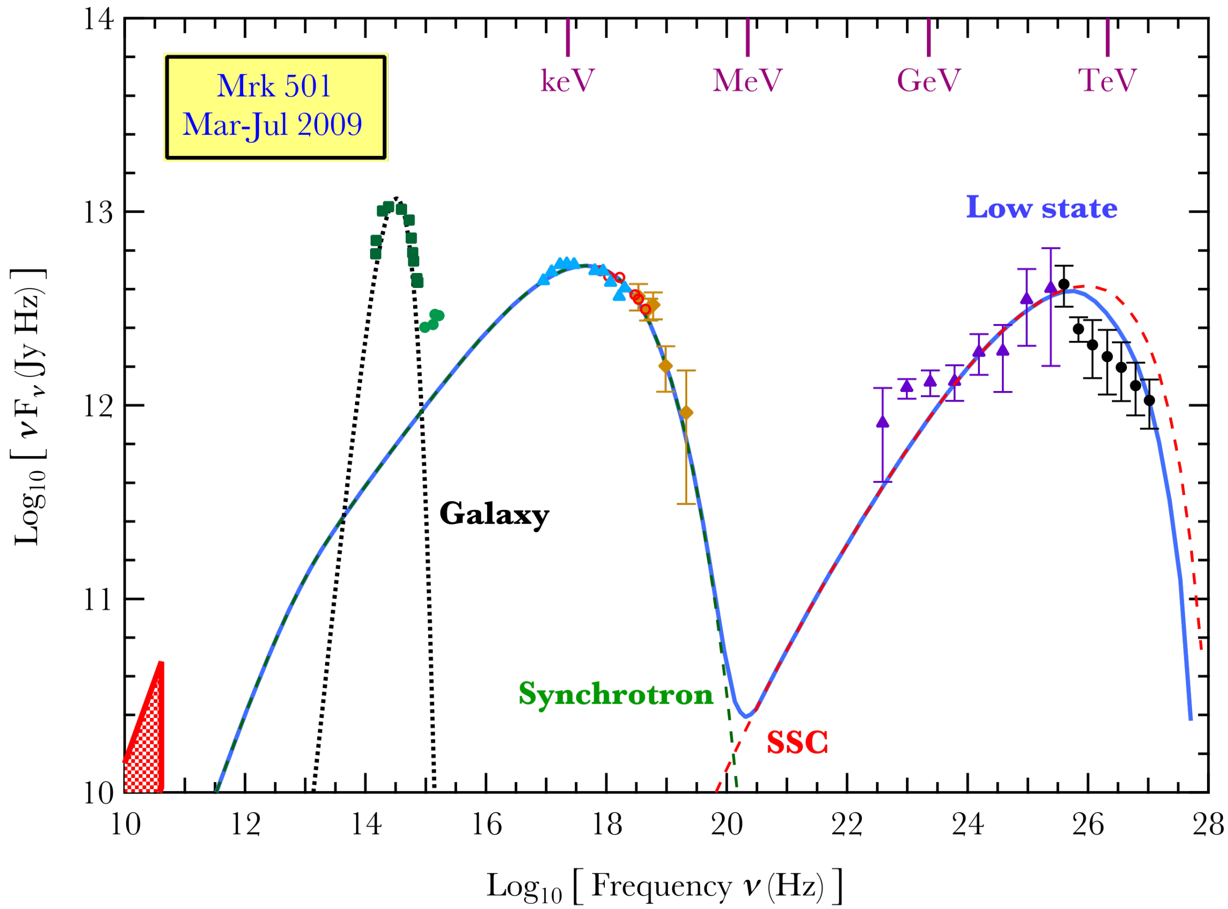

Baring, Boettcher & Summerlin (2017, MNRAS): steady-state models only

z=0.034

η_1=100
α = 3/2

- Synchrotron explains X-rays but cannot fit optical/UV; galaxy component added.
- Large η (~10^4) needed to move synchrotron peak $E_{max} \sim m_e c^2/(\eta \alpha_f)$ into X-rays.
- Need for large $\eta = \lambda / r_g$ in blazars identified by Inoue & Takahara (1996).

Shock Acceleration Injection Efficiencies

$\eta(p) = \lambda/r_g \sim \eta_1\,(p/mc)^{\alpha-1}$

Baring et al. (MNRAS, 2017)

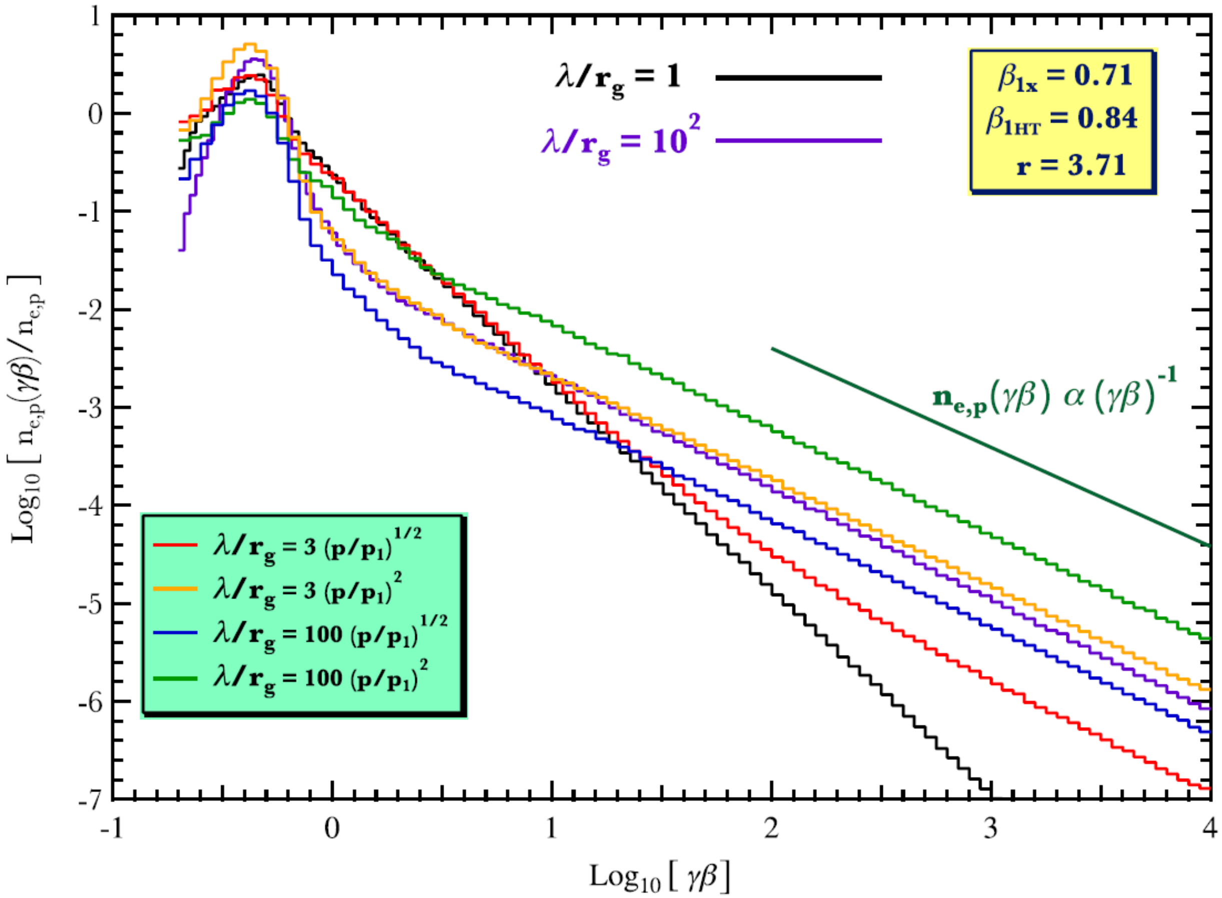

- **The non-thermal particle spectral index and thermal-to-non-thermal normalization from Monte Carlo acceleration simulations are strongly dependent on** η_1 (=3,100 in the figure) **and** α (=1/2, 2 in figure), **and the B-field obliquity to the shock normal!**

Constraining SSC fit Parameter $\eta=\lambda_{||}/r_g$

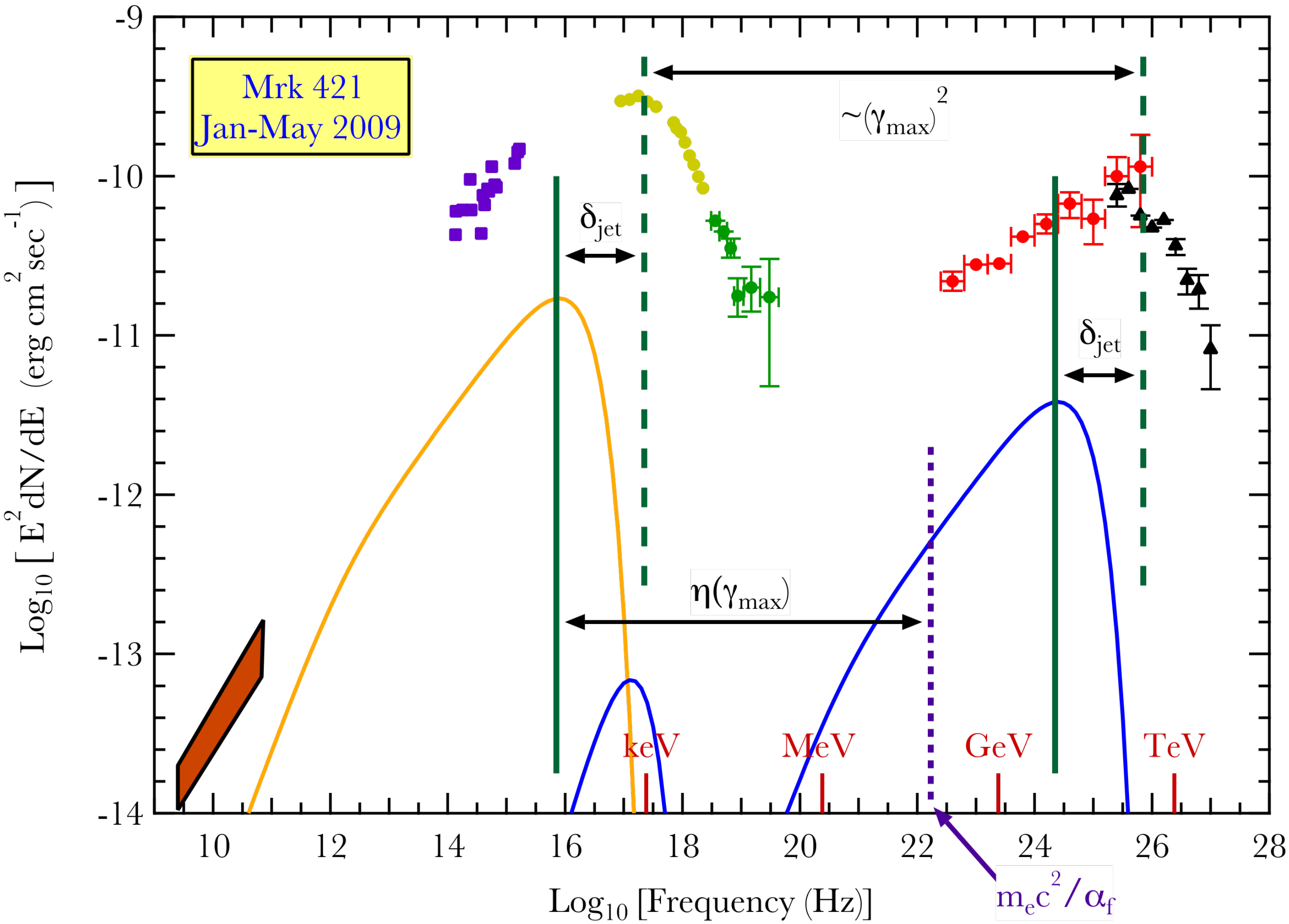

- Large η needed to move synchrotron peak $E_{max} \sim m_e c^2/(\eta \alpha_f)$ into X-rays.

Canonical Turbulence Power Spectrum

- Inertial range can span 1-5 orders of magnitude.
- Doppler gyro-resonance condition $\omega = \Omega/\gamma$ may not be satisfied by charges with large gyroradii;
- => increase of diffusive mean free path parameter $\eta = \lambda/r_g$ at large momenta.
- Expect $\lambda \propto p^2$ at long wavelengths, below stirring scale (QLT).